Structure
Article

Structural Biology of RNA Polymerase III: Mass Spectrometry Elucidates Subcomplex Architecture

Kristina Lorenzen,[1] Alessandro Vannini,[2] Patrick Cramer,[2] and Albert J.R. Heck[1,*]
[1]Department of Biomolecular Mass Spectrometry, Bijvoet Center for Biomolecular Research and Utrecht Institute for Chemistry, Utrecht University, Sorbonnelaan 16, 3584 CA Utrecht, The Netherlands
[2]Gene Center Munich and Center for Integrated Protein Science CiPSM, Department of Chemistry and Biochemistry, Ludwig-Maximilians-Universität München, Feodor-Lynen-Strasse 25, 81377 Munich, Germany
*Correspondence: a.j.r.heck@uu.nl
DOI 10.1016/j.str.2007.07.016

SUMMARY

RNA polymerases (Pol) II and III synthesize eukaryotic mRNAs and tRNAs, respectively. The crystal structure of the 12 subunit Pol II is known, but only limited structural information is available for the 17 subunit Pol III. Using mass spectrometry (MS), we correlated masses of Pol II complexes with the Pol II structure. Analysis of Pol III showed that the complete enzyme contains a single copy of each subunit and revealed a 15 subunit form lacking the Pol III-specific subcomplex C53/37. DMSO treatment dissociated the C17/25 heterodimer of Pol III, confirming a peripheral location as its counterpart in Pol II. Tandem MS revealed the Pol III-specific subunits C82 and C34 dissociating as a heterodimer. C11 was retained, arguing against a stable trimeric subcomplex, C53/37/11. These data suggest that Pol III consists of a 10 subunit Pol II-like core; the peripheral heterodimers C17/25, C53/37, and C82/34; and subunit C31, which bridges between C82/34, C17/25, and the core.

INTRODUCTION

The multisubunit RNA polymerases (Pols) I, II, and III synthesize eukaryotic RNA during gene transcription. Pol I and Pol II synthesize ribosomal and mainly messenger RNA, respectively, and Pol III transcribes small RNAs, including transfer RNAs (tRNAs), 5S ribosomal RNA, and U6 small nuclear RNA. The size and complexity of the polymerases increase from Pol II (12 subunits, 514 kDa) via Pol I (14 subunits, 588 kDa) to Pol III (17 subunits, 693 kDa). Detailed structural information, including the crystal structures of the 10 subunit core enzyme (Cramer et al., 2000, 2001), the additional subcomplex Rpb4/7, and the complete 12 subunit enzyme, is available for Pol II (Armache et al., 2003, 2005; Bushnell and Kornberg, 2003). These structures provide a framework for understanding the subunit architecture of the two other polymerases.

Open questions remain, particularly for the subunit architecture of Pol III, since it is the most complex enzyme (Chedin et al., 1998; Geiduschek and Kassavetis, 2001; Schramm and Hernandez, 2002). Pol III apparently contains a 10 subunit core homologous to Pol II. The C17/25 subcomplex it comprises is the counterpart of the Rpb4/7 subcomplex in Pol II, and, in addition, it contains the five additional subunits C82, C53, C37, C34, and C31. The C17/25 subcomplex constitutes a stalk that protrudes from the polymerase core, is involved in the initiation of transcription via recognition of promoter-bound factors, and may bind exiting RNA (Dezelee et al., 1976; Jasiak et al., 2006). In Pol II, Rpb4/7 can dissociate from the core as a heterodimer, but it remained unclear if C17/25, as the homolog counterpart in Pol III, shows this behavior as well. Subunits C82, C34, and C31 form a stable trimeric subcomplex in isolation (Wang and Roeder, 1997; Werner et al., 1992), but it is unknown if and how the C82/34/31 subcomplex can dissociate from the core. C53 and C37 form a heterodimer and are important for terminator recognition (Landrieux et al., 2006). C53/37, together with C11, also plays a key role in facilitated reinitiation. Subunit C11 is involved in the intrinsic RNA-cleavage activity of Pol III (Chedin et al., 1998) and shows sequence similarity with the Pol II subunit Rpb9 and the elongation factor TFIIS. It has been suggested that the Pol III-specific subunits C53 and C37, together with C11, belong to an autonomous structural module, based on the fact that mutations in either C37 or C11 lead to the loss of C53, C37, and C11 after Pol III purification (Hu et al., 2002; Landrieux et al., 2006). This is difficult to reconcile with the idea that C11 is part of a conserved structural core, and association of these three subunits in isolation has not been demonstrated. The recent electron microscopic analysis of Pol III indicated that the C82/34/31 subcomplex is located mainly on one side above the central DNA-binding cleft, whereas the C53/37 subcomplex may be situated across the cleft on the side of the enzyme (Fernandez-Tornero et al., 2007). It also remains unclear if all cellular Pol III exists as an intact 17 subunit complex, or if other species coexist that lack particular subunits or subcomplexes and possibly differ in their function (Ferri et al., 2000; Huet et al., 1985).

Here, we address open questions on the Pol III architecture by analyzing multisubunit RNA polymerases and their

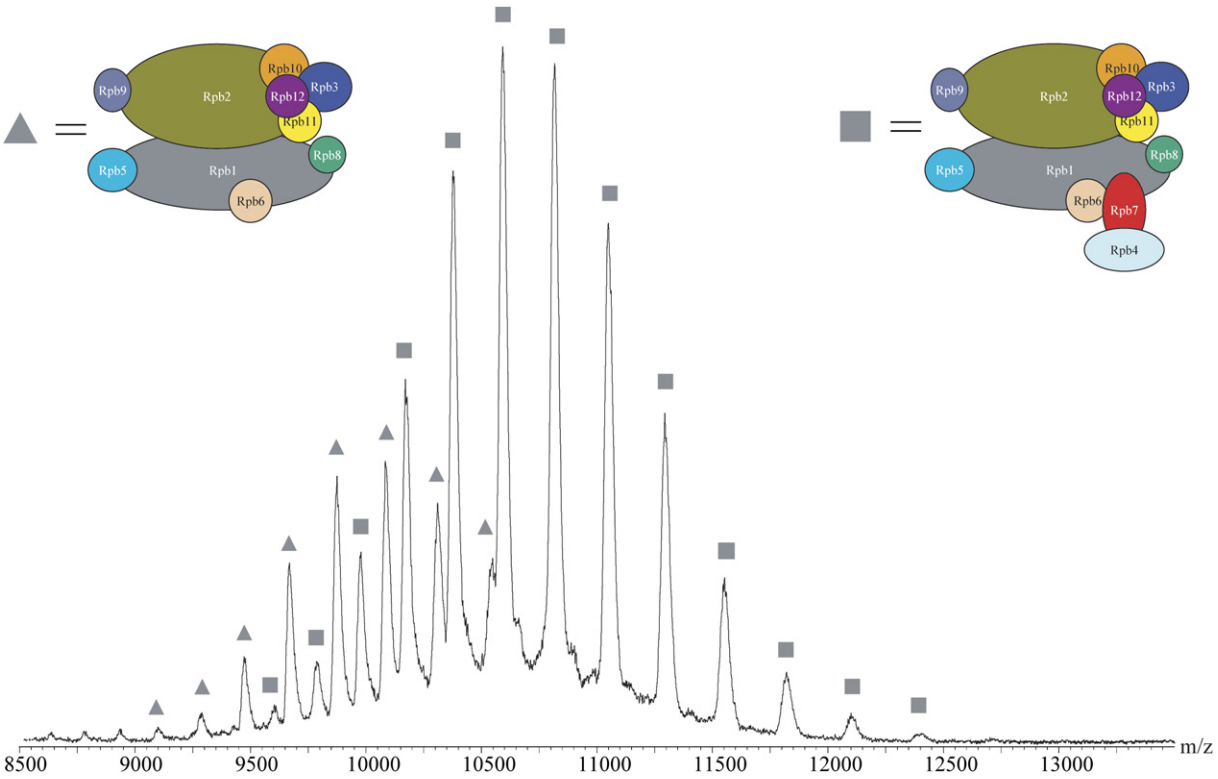

Figure 1. Native Mass Spectrum of the Purified Pol II Complexes

The two different charge distributions reveal two distinct complex stoichiometries. The squares indicate the charge distribution of the complete 12 subunit protein complex with a mass of 517 kDa. The triangles indicate the charge distribution of the complex missing Rpb4 and Rpb7 (472 kDa). The insets show structural models of the proposed complexes.

subcomplexes by native mass spectrometry. To establish the experimental approach, we analyzed Pol II and correlated the mass spectrometric data with known structural information. Application of this method to Pol III provided insights into the architecture of this enzyme. Our results not only provide insights into the subunit architecture of the largest cellular RNA polymerase, but they also indicate that it may become feasible to study functional complexes of endogenously expressed RNA polymerases by mass spectrometry.

RESULTS

Mass Spectrometry of Pol II Detects the Two Known Forms of the Enzyme

Macromolecular mass spectrometry (Heck and Van Den Heuvel, 2004; Ilag et al., 2004; Robinson, 2002; van den Heuvel and Heck, 2004; van Duijn et al., 2005) can be used to detect and measure the masses of large, multicomponent complexes, such as ribosomes and exosomes (Hernandez et al., 2006; McKay et al., 2006; Synowsky et al., 2006), but it has not been shown to be applicable to the multisubunit RNA polymerases. Figure 1 shows a mass spectrum of a preparation of endogenous Pol II from the yeast *Saccharomyces cerevisiae*. In the spectrum, two charge distributions can be distinguished in the range from 9,000 to 13,000 m/z, that allow for the deduction of the masses of the underlying complexes. The species with the highest mass is most abundant, accounting for 66% of the total ion intensity, and has a mass of 517,320 ± 140 Da. This mass fits well with the expected mass of the intact, complete 12 subunit Pol II (513,540 Da). For very large complexes, the masses measured in macromolecular mass spectrometry are typically higher than the expected masses since desolvation is generally incomplete, leaving additional water and buffer molecules attached to the protein complex (McKay et al., 2006). The second species has a mass of 472,720 ± 120 Da, giving a measured mass difference between the two Pol II species of 44,600 Da. This difference corresponds very well to the sum of the masses of subunits Rpb4 and Rpb7 (44,530 Da). The co-occurrence of this second complex may be expected since Rpb4 and Rpb7 can dissociate from Pol II as a heterodimer. Thus, the second species corresponds to the 10 subunit Pol II core enzyme.

Stoichiometry of Pol III and a Pol III Form Lacking C53/37

We recorded the macromolecular mass spectra of a preparation of endogenous yeast Pol III under similar experimental settings as for Pol II. The mass spectra also displayed more than one species (Figure 2). Better-resolved

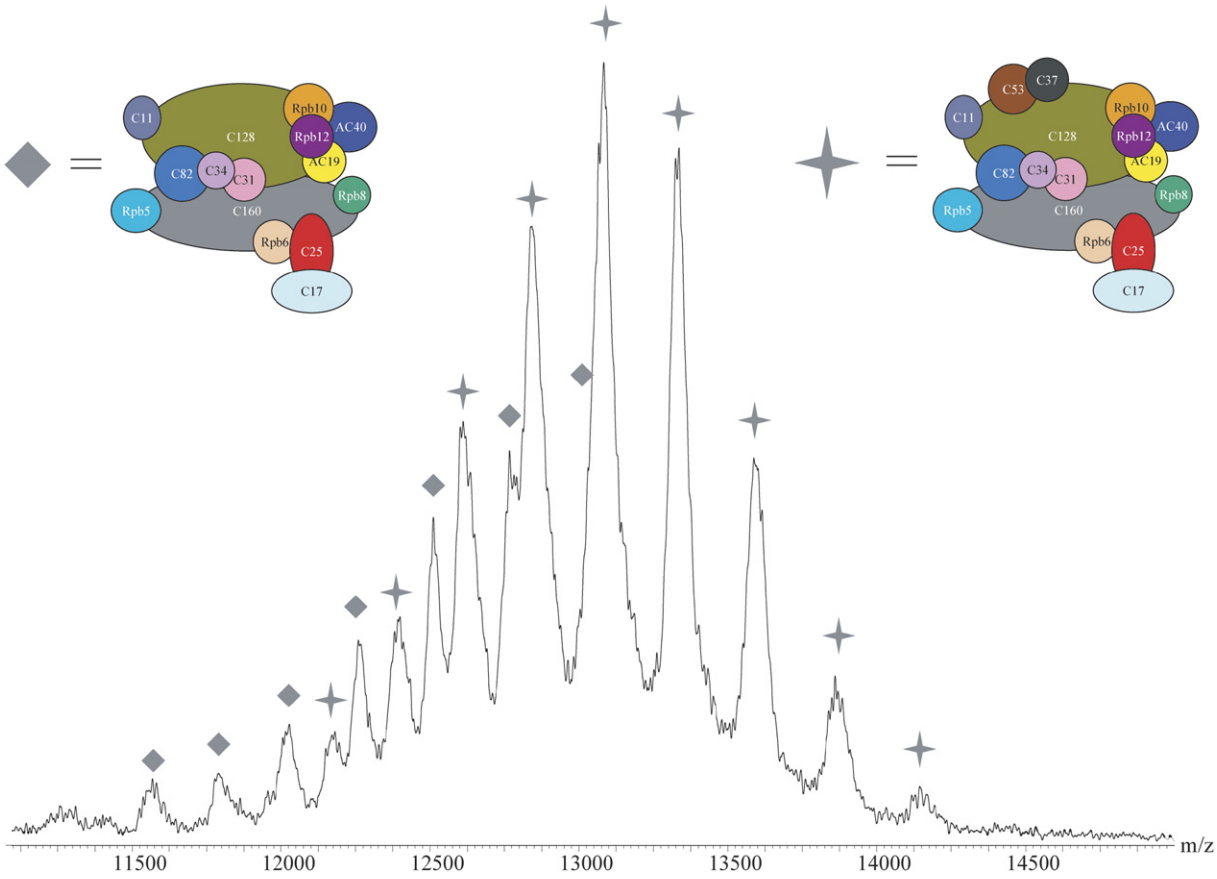

Figure 2. Native Mass Spectrum of the Purified Pol III Complexes

The two different charge distributions reveal two distinct complex stoichiometries. The stars indicate the charge distribution of the complete 17 subunit Pol III complex with a mass of 699 kDa. The diamonds mark the charge distribution of the complex missing the subunits C53 and C37 (620 kDa). The insets show structural models of the proposed complexes.

spectra at a higher desolvation energy showed that the main species had a mass of 699,180 ± 120 Da, which corresponds well with the expected mass of the intact, complete 17 subunit Pol III if a single copy of each subunit is assumed to be present (693,230 Da). A second, distinct charge distribution revealed a subcomplex with a mass of 620,320 ± 130 Da. The difference in mass between these two species is 78,860 Da, which is consistent with the second complex missing C53 and C37 (expected mass 78,800 Da). To make sure that this was not an artifact due to degraded forms of C53 in the purification that could fall apart under conditions used for mass spectroscopy, we checked the purification on an SDS gel (Figure S6; see the Supplemental Data available with this article online). There were no degraded forms of C53 visible. Additionally, it has been described in previous studies that subunit C53 occurs at substoichiometric levels upon Pol III purification (Sadhale and Woychik, 1994; Sentenac, 1985). In our measurements, the intact Pol III was more abundant in the spectrum and accounted for 66% of the ion intensity. At high desolvation energy, a small amount of complex that lost only the subunit C53, and still retained C37, could be detected (see Figure S1). An overview of all measured masses and the protein homologies between Pol II and Pol III is summarized in Table 1. A comparison between the masses detected and theoretical masses derived from the protein sequence is given in Table S1. To confirm that the different subcomplexes of Pol III are not a mass spectrometric artifact and are not due to the buffer exchange to ammonium acetate, native PAGE, which clearly showed two different bands for the two protein complexes (data not shown), was carried out.

Peripheral Subunits in Pol II and Pol III

To probe which subunits are positioned at the surface of Pol II and Pol III, we gently dissociated the polymerase complexes in solution by adding low percentages of organic modifiers to the aqueous ammonium acetate electrospray solutions (Hernandez et al., 2006). By adding from 1% to 10% DMSO, we observed charge distributions of several subunits and a few subcomplexes in the low-mass range (Table 2). For Pol II, we detected ions originating from subunits Rpb4, Rpb5, Rpb6, Rpb7, Rpb8, Rpb9, and Rpb12. The mass detected for Rpb9 was 65 Da higher than expected, showing that one of the two zinc ions in Rpb9 was still bound to the subunit. In addition, we

Table 1. Overview of Polymerase Subunits and Their Homologies

Polymerase Part	Pol III Subunit	Masses Detected (Da)	Pol II Subunit	Masses Detected (Da)	Subunit Type
Core	C160	—[a]	Rpb1	—	homolog
	C128	—	Rpb2	—	homolog
	AC40	37,603 ± 5	Rpb3	—	homolog
	AC19	16,024 ± 4	Rpb11	13,660 ± 3	homolog
	Rpb5	25,124 ± 4	Rpb5	25,127 ± 5	common
	Rpb6	17,902 ± 3	Rpb6	17,902 ± 3	common
	Rpb8	16,425 ± 4	Rpb8	16,425 ± 4	common
	Rpb10	8,280 ± 1	Rpb10	8,280 ± 1	common
	Rpb12	7,692 ± 1	Rpb12	7,692 ± 1	common
	C11[b]	12,639 ± 2	Rpb9	14,265 ± 3	homolog
Rpb4/7/C17/25 heterodimer	C17	18,530 ± 4	Rpb4	25,460 ± 6	counterpart
	C25	24,330 ± 4	Rpb7	19,062 ± 5	counterpart
C53/37 heterodimer	C53	—	—	—	specific
	C37	32,009 ± 5	—	—	specific
Upstream heterotrimer	C82	74,075 ± 8	—	—	specific
	C34	36,052 ± 5	—	—	specific
	C31	—	—	—	specific
Intact complex		699,180 ± 120		517,320 ± 140	
Subcomplex		620,320 ± 130		472,720 ± 120	
Rpb4/7/C17/25 heterodimer		42,846 ± 7		44,526 ± 10	
C82/34 heterodimer		110,130 ± 20			

Listed next to the subunit is the mass that was detected for this subunit during the experiments. The masses of the detected complexes and subcomplexes are indicated in the bottom section of the table.
[a] The em dash indicates that the mass was not detected.
[b] Rpb9 was previously defined as a part of the Pol II core. C11 shows homology to Rpb9 and TFIIS.

detected the intact Rpb4/7 heterodimer. All of these subunits are located on the Pol II surface in the X-ray structure. Interestingly, subunits Rpb3, Rpb10, and Rpb11 were not dissociated, in agreement with their proposed role as an assembly nucleus that anchors the two large subunits, and consistent with Rpb1, Rpb2, Rpb3, and Rpb11 forming the evolutionarily conserved core that is also found in the bacterial RNA polymerase. Thus, the DMSO dissociation experiments yield valuable insights into subunit architecture and complex stability. The same treatment of the Pol III complex resulted in dissociation of subunits homologous to the dissociating Pol II subunits (Table 2). For C11, the counterpart to Rpb9, a mass was detected that was 130 Da higher than expected, suggesting that two predicted structural zinc ions remained bound to the subunit. The spectra also revealed the C17/25 heterodimer, which corresponds to Rpb4/7 in Pol II, underlining the similarity in the architecture of the Pol II and Pol III complexes. Additionally, we detected signals for C82 and C34 as well as a signal of low intensity assigned to C37. These experiments also revealed a likely abundant single phosphorylation in Rpb6 in both polymerases that may serve a common function; Rpb6 was detected with a mass of 17,902 Da as well as with a mass that is 80 Da higher (17,982 Da) (Table 2).

Tandem Mass Spectrometry of Pol II and Pol III

To further investigate the architecture of the Pol II and Pol III complexes and their coexisting subcomplexes, we employed tandem mass spectrometry (McCammon et al., 2004; van Duijn et al., 2006). During the transfer of proteins into the mass spectrometer, protonation leads to the presence of the protein in different charge states. Tandem mass spectrometry allows for the selection of one charge state of the subset precursor complexes, which can be collisionally activated in the mass spectrometer, resulting in specific dissociation. In these experiments, the precursor ions generally eliminate a single subunit, which will become highly charged, concomitant with the formation of relatively low-charged ions of the precursor complex lacking the eliminated subunit (Heck and Van Den Heuvel, 2004). Evidently, the summed mass and charge of the two formed fragment ions should add up to the mass and charge of the precursor complex. Elimination of different

Table 2. List of Subunits that Dissociated from the Polymerases as a Result of the DMSO Treatment

Pol III Subunit	Detection State	Pol II Subunit	Detection State
C160	—[a]	Rpb1	—
C128	—	Rpb2	—
AC40	—	Rpb3	—
AC19	—	Rpb11	—
Rpb5	x[b]	Rpb5	x
Rpb6	x	Rpb6	x
Rpb6[c]	x	Rpb6[c]	x
Rpb8	x	Rpb8	x
Rpb10	—	Rpb10	—
Rpb12	x	Rpb12	x
C11[d]	x	Rpb9[e]	x
C17	x	Rpb4	x
C25	x	Rpb7	x
C53	—		
C37	x		
C82	x		
C34	x		
C31	—		
C17/25 heterodimer	x	Rpb4/7 heterodimer	x

[a] The em dash indicates that the subunit was not found.
[b] An "x" indicates that the subunit was detected.
[c] Rpb6 was additionally detected with a mass difference of an additional 80 Da.
[d] C11 was detected with a mass difference of an additional 130 kDa.
[e] Rpb9 was detected with a mass difference of an additional 65 kDa.

protein subunits may occur in parallel and sequentially. We performed tandem mass spectrometry by selecting charge states originating either from the complete Pol II or Pol III, or from their subcomplexes that had lost the Rpb4/7 or C53/37 heterodimer, respectively.

Tandem Mass Spectrometry Patterns Reflect the Pol II Architecture

Tandem mass spectrometry on the complete Pol II (517 kDa) led primarily to the elimination of subunits Rpb4 and Rpb7 and the intact Rpb4/7 heterodimer (Table 3; and Figure S2). Elimination of protein dimers is rarely observed in tandem mass spectrometry of protein complexes, since subunits often unfold upon dissociation. However, observation of the Rpb4/7 heterodimer is not so surprising since it forms a stable subcomplex in vivo. The concomitant high-mass fragment ions of the complexes could be assigned to the ΔRpb4, ΔRpb7, and ΔRpb4/7 complexes. These results reflect the known biochemical and structural data on the architecture of Pol II. It has been observed before that structures can be partially retained in the gas phase (Ruotolo and Robinson, 2006; van Duijn et al., 2005). Other single subunits that were detected were Rpb12 and, at higher collision energy, Rpb10. The Pol II complexes ΔRpb12 and ΔRpb10 were not visible; likely, their signal was suppressed or too weak compared to the strong signal of the ΔRpb4/7 complex. Tandem mass spectrometry at higher energy of the Pol II core complex lacking Rpb4/7 revealed additional dissociation products (Figure S3). Monomeric ions of the surface subunits Rpb5, Rpb8, Rpb9, Rpb10, Rpb11, and Rpb12 were eliminated. For most of the dissociated subunits, the concomitant remaining complexes could be assigned. The ΔRpb12 and complexes that lacked Rpb10 were found. The ΔRpb8 complex could be dissociated further, resulting in complexes lacking Rpb8 and either Rpb11, Rpb5, or Rpb9. Since no Pol II complexe ΔRpb4 or ΔRpb7 was observed, we conclude that, indeed, the initial Pol II subcomplex corresponds to the 10 subunit core.

The Pol III Core Architecture Resembles that of Pol II

The complete Pol III and the presumed ΔC53/37 complex showed a similar pattern of subunit elimination in tandem mass spectrometry (Figures S4 and S5). For both complexes, 9 out of the 17 Pol III subunits were detected as monomeric fragment ions (Table 3). The common and homologous subunits that were eliminated during the tandem mass spectrometry of the Pol II core complex were all found to dissociate from the Pol III complexes as well, with

Table 3. Subunits Eliminated from the Different Polymerase Complexes

	Pol III			Pol II	
	699 kDa	620 kDa		517 kDa	472 kDa
C160	—[a]	—	Rpb1	—	—
C128	—	—	Rpb2	—	—
AC40	x[b]	x	Rpb3	—	—
AC19	x	x	Rpb11	—	x
Rpb5	—	—	Rpb5	—	x
Rpb6	—	—	Rpb6	—	—
Rpb8	x	x	Rpb8	—	x
Rpb10	x	x	Rpb10	x	x
Rpb12	x	x	Rpb12	x	x
C11	—	—	Rpb9	—	x
C17	x	x	Rpb4[c]	x	
C25	x	x	Rpb7[c]	x	
C53	—	—	—		
C37	—	—	—		
C82	x	x	—		
C34	x	x	—		
C31	—	—	—		
C82/34 subcomplex	x	x	Rpb4/7 subcomplex	x	

The complex from which each subunit dissociated is indicated at the top of the table. The masses that were assigned to each subunit are listed in Table 1.
[a] The em dash indicates that the subunit was not found.
[b] An "x" indicates that the subunit was detected during the measurement.
[c] Due to contamination of the 517 kDa Pol II species in the tandem MS of the 472 kDa subcomplex, there were small amounts of Rpb4 and Rpb7 detected in the spectrum.

the exception of Rpb5. All concomitant high-mass fragments that were detected for the complete Pol III (699 kDa) still included the mass of C37 and C53, indicating that these subunits are quite stably associated with Pol III and do not dissociate from the complex under the conditions used. The subunits that were found to dissociate from Pol III only leave Rpb5, Rpb6, C11, C37, C53, and C31 to account for the missing mass between the complete Pol III and its smaller subcomplex. The only combination that fits the experimental mass difference (78,870 Da) between the complete Pol III and the smaller complex of Pol III is that of C37 and C53, supporting the notion that a discrete ΔC53/37 complex of Pol III is present in the preparation.

A Peripheral C82/34 Heterodimer Can Dissociate from Pol III

A striking difference between tandem mass spectrometry of Pol III and Pol II is the elimination of a Pol III-specific C82/34 heterodimer. We detected fragment ions of a mass of 110,130 Da, corresponding very well to the theoretical (as given in Table 1) combined mass of C82 and C34 (110,130 Da). These fragment ions were observed in tandem mass spectra of both the complete Pol III and the subcomplex lacking C37/53 (Figure 3). The concomitant high-mass fragments could also be detected and mass assigned, confirming dissociation of a C82/34 heterodimer and retention of C31 in the remaining polymerase complex. These data cannot completely exclude the existence of a C82/34/31 heterotrimer that was described previously (Hu et al., 2002; Landrieux et al., 2006). Instead, they indicate that the interaction of C31 with the polymerase in the gas phase is tighter than its interaction with the C82/34 heterodimer. As for the stable Rpb4/7 heterodimer in Pol II, C82 and C34 were also detected as fragment ions. Another difference between Pol II and Pol III concerns an apparently different stability of the assembly core. The Pol III subunits AC40 and AC19 were detected as fragment ions in tandem mass spectrometry, whereas the Pol II homolog Rpb3 did not dissociate from Pol II. AC19 dissociates with a mass of 16,024 Da and with a mass of 16,104 Da, revealing a potential phosphorylation site in Pol III.

DISCUSSION

Here, we have used native mass spectrometry to analyze the architecture of the multisubunit RNA polymerases

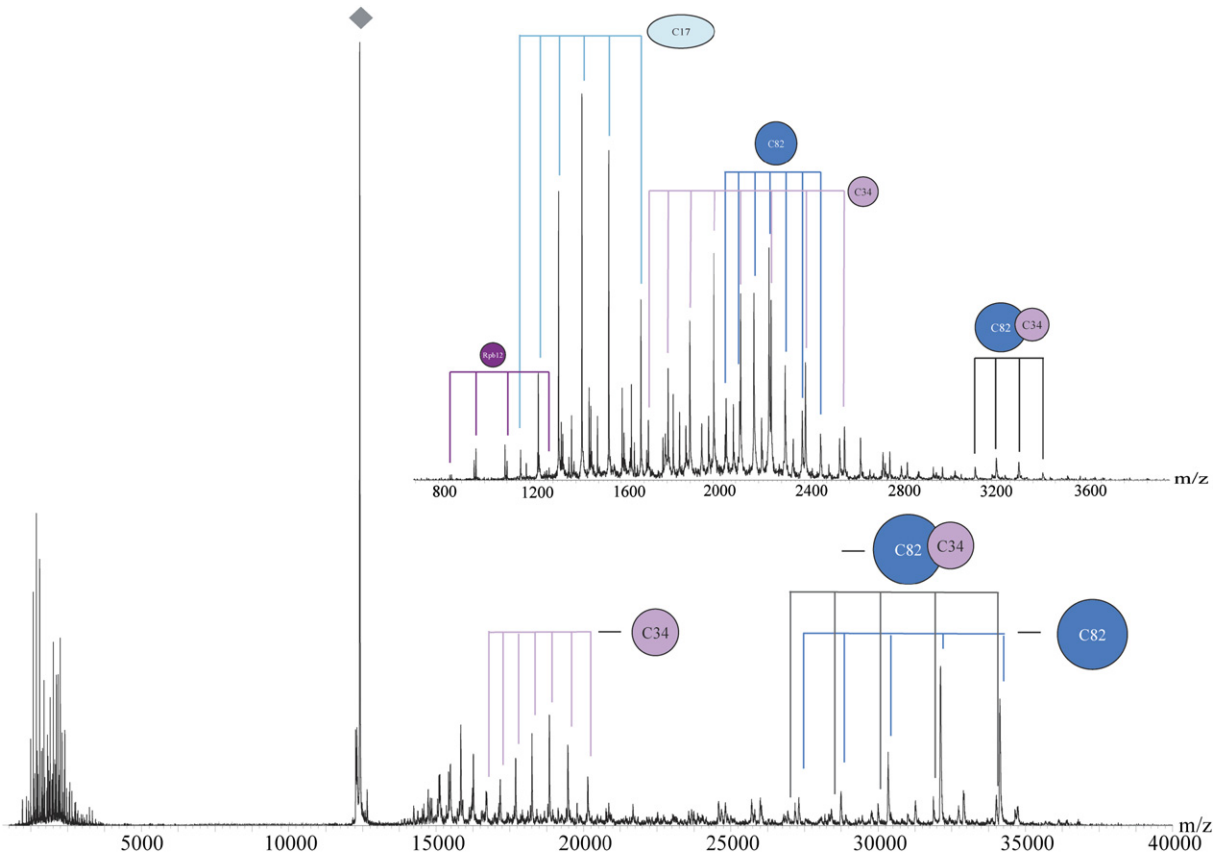

Figure 3. Tandem Mass Spectrum of the 620 kDa Subcomplex of Pol III

The 50+ charge state of the complex was selected for collisional activation, indicated with a diamond. The spectrum reveals the dissociation of the C82/34 dimer. Above m/z 12,000, the distributions representing the subcomplex that eliminated C34, C82, or its heterodimer are labeled. The zoom-in at the low-m/z region reveals subunits that were eliminated from the complex. The dimer of C82/34 is visible.

Pol II and Pol III. Our results reveal different forms of Pol II and Pol III in solution. With the use of DMSO treatment and tandem mass spectrometry, peripheral subcomplexes could be dissociated from the enzymes and could be identified. Our results have two major implications. First, they demonstrate the technical feasibility of studying multisubunit RNA polymerases by native mass spectrometry. The validity of this approach is demonstrated by successful correlation of the observed masses for Pol II and its subunits and subcomplexes to the known three-dimensional structure. In the future, it may be possible to study the formation and stability of functional complexes of RNA polymerases with mass spectrometry. Second, our results provide important insights into the subunit architecture of Pol III, the largest cellular RNA polymerase, which comprises five additional, specific subunits arranged in specific subcomplexes. The data demonstrate that each of the 17 subunits of Pol III is present as a single copy. Pol III apparently comprises a 10 subunit core that resembles the structure of the Pol II core and apparently includes subunit C11, even though a trimeric subcomplex, C53/37/11, as suggested previously, cannot be completely ruled out. Arrayed around the periphery of the core are three heterodimeric subcomplexes, C53/37, C82/34, and C17/25; the latter one corresponds to Rpb4/7 in Pol II. Subunit C31 binds to the Pol III core and to subunit C17 (Chedin et al., 1998; Geiduschek and Kassavetis, 2001; Schramm and Hernandez, 2002), but it has also been shown to form a stable trimer with C82 and C34 (Wang and Roeder, 1997; Werner et al., 1992), suggesting that it is involved in bridging between C82/34, the core, and C17/25. The obtained model for the Pol III subunit architecture will guide future biochemical and structural studies of this central cellular enzyme.

EXPERIMENTAL PROCEDURES

Purification of Pol II and Pol III

Pol II was purified as described previously (Brueckner et al., 2007). Pol III was purified as described (Figure S6) (Kassavetis et al., 1990).

Mass Spectrometry of Pol II and Pol III

The sample buffer was exchanged sequentially to 200 mM (Pol II) or 400 mM (Pol III) aqueous ammonium acetate (pH 6.8) by using centrifugal filter units with a cutoff of 100 kDa (Millipore, England). The concentration used for the mass spectrometry measurements was ~2 μM (assuming intact protein complexes). The samples were measured on a LCT electrospray time-of-flight instrument for the DMSO measurements and on a modified Q-ToF electrospray quadrupole time-of-flight instrument for native mass spectrometry and tandem mass

spectrometry (van den Heuvel et al., 2006) (Waters, Manchester, UK). Nanospray glass capillaries were used to introduce the samples into the Z-spray source. The source pressure was increased to 10 mbar to create increased collisional cooling (Krutchinsky et al., 1998; Tahallah et al., 2001). Source temperature was set to 80°C, and sample cone voltage varied from 125 to 175 V. Needle voltage was ~1300 V in the case of the LCT instrument and ~1600 V for the Q-ToF instrument.

For the tandem mass spectrometry measurements, precursor ions of specific m/z were selected in the quadrupole. Subsequently, they were accelerated through the collision cell by applying voltages from 0 to 200 V over this cell. Xenon was used as the collision gas in the MS/MS experiments to increase ion transmission and energy-transfer efficiency during the process (Lorenzen et al., 2007). Pressure conditions were 1.5×10^{-2} mbar in the collision cell and 2.3×10^{-6} mbar in the ToF. The faults indicated in the measurements are calculated from the variability of the different charge states. For each charge state, a mass is calculated, and the masses are averaged and the standard deviation is calculated. The masses measured during repetition of the experiments were within these deviations. The sequence masses given in Figure S1 have been taken from the SWISS-PROT database (Bairoch and Apweller, 1997) (http://www.expasy.org/).

Supplemental Data

Supplemental Data include a resolved mass spectrum of Pol III at 150 V collision energy (Figure S1), tandem mass spectra of the Pol II and III (sub) complexes (Figures S2–S5), an SDS gel of purified Pol III (Figure S6), and a comparison between the measured and theoretical masses based on the sequence (Table S1) and are available at http://www.structure.org/cgi/content/full/15/10/1237/DC1/.

ACKNOWLEDGMENTS

This work was supported by a European Molecular Biology Organization long-term fellowship and by the Netherlands Proteomics Centre.

Received: April 27, 2007
Revised: July 9, 2007
Accepted: July 31, 2007
Published: October 16, 2007

REFERENCES

Armache, K.J., Kettenberger, H., and Cramer, P. (2003). Architecture of initiation-competent 12-subunit RNA polymerase II. Proc. Natl. Acad. Sci. USA *100*, 6964–6968.

Armache, K.J., Mitterweger, S., Meinhart, A., and Cramer, P. (2005). Structures of complete RNA polymerase II and its subcomplex, Rpb4/7. J. Biol. Chem. *280*, 7131–7134.

Bairoch, A., and Apweller, R. (1997). The SWISS-PROT protein sequence data bank and its supplement TrEMBL. Nucleic Acids Res. *25*, 31–36.

Brueckner, F., Hennecke, U., Carell, T., and Cramer, P. (2007). CPD damage recognition by transcribing RNA polymerase II. Science *315*, 859–862.

Bushnell, D.A., and Kornberg, R.D. (2003). Complete, 12-subunit RNA polymerase II at 4.1-Å resolution: implications for the initiation of transcription. Proc. Natl. Acad. Sci. USA *100*, 6969–6973.

Chedin, S., Ferri, M.L., Peyroche, G., Andrau, J.C., Jourdain, S., Lefebvre, O., Werner, M., Carles, C., and Sentenac, A. (1998). The yeast RNA polymerase III transcription machinery: a paradigm for eukaryotic gene activation. Cold Spring Harb. Symp. Quant. Biol. *63*, 381–389.

Cramer, P., Bushnell, D.A., Fu, J., Gnatt, A.L., Maier-Davis, B., Thompson, N.E., Burgess, R.R., Edwards, A.M., David, P.R., and Kornberg, R.D. (2000). Architecture of RNA polymerase II and implications for the transcription mechanism. Science *288*, 640–649.

Cramer, P., Bushnell, D.A., and Kornberg, R.D. (2001). Structural basis of transcription: RNA polymerase II at 2.8 Å resolution. Science *292*, 1863–1876.

Dezelee, S., Wyers, F., Sentenac, A., and Fromageot, P. (1976). Two forms of RNA polymerase B in yeast. Proteolytic conversion in vitro of enzyme BI into BII. Eur. J. Biochem. *65*, 543–552.

Fernandez-Tornero, C., Bottcher, B., Riva, M., Carles, C., Steuerwald, U., Ruigrok, R.W., Sentenac, A., Muller, C.W., and Schoehn, G. (2007). Insights into transcription initiation and termination from the electron microscopy structure of yeast RNA polymerase III. Mol. Cell *25*, 813–823.

Ferri, M.-L., Peyroche, G., Siaut, M., Lefebvre, O., Carles, C., Conesa, C., and Sentenac, A. (2000). A novel subunit of yeast RNA polymerase III interacts with the TFIIB-related domain of TFIIIB70. Mol. Cell. Biol. *20*, 488–495.

Geiduschek, E.P., and Kassavetis, G.A. (2001). The RNA polymerase III transcription apparatus. J. Mol. Biol. *310*, 1–26.

Heck, A.J., and Van Den Heuvel, R.H. (2004). Investigation of intact protein complexes by mass spectrometry. Mass Spectrom. Rev. *23*, 368–389.

Hernandez, H., Dziembowski, A., Taverner, T., Seraphin, B., and Robinson, C.V. (2006). Subunit architecture of multimeric complexes isolated directly from cells. EMBO Rep. *7*, 605–610.

Hu, P., Wu, S., Sun, Y., Yuan, C.C., Kobayashi, R., Myers, M.P., and Hernandez, N. (2002). Characterization of human RNA polymerase III identifies orthologues for *Saccharomyces cerevisiae* RNA polymerase III subunits. Mol. Cell. Biol. *22*, 8044–8055.

Huet, J., Riva, M., Sentenac, A., and Fromageot, P. (1985). Yeast RNA polymerase C and its subunits. Specific antibodies as structural and functional probes. J. Biol. Chem. *260*, 15304–15310.

Ilag, L.L., Westblade, L.F., Deshayes, C., Kolb, A., Busby, S.J.W., and Robinson, C.V. (2004). Mass spectrometry of *Escherichia coli* RNA polymerase: interactions of the core enzyme with [σ]70 and Rsd protein. Structure *12*, 269–275.

Jasiak, A.J., Armache, K.J., Martens, B., Jansen, R.P., and Cramer, P. (2006). Structural biology of RNA polymerase III: subcomplex C17/25 X-ray structure and 11 subunit enzyme model. Mol. Cell *23*, 71–81.

Kassavetis, G.A., Braun, B.R., Nguyen, L.H., and Geiduschek, E.P. (1990). *S. cerevisiae* TFIIIB is the transcription initiation-factor proper of RNA polymerase III, while TFIIIA and TFIIIC are assembly factors. Cell *60*, 235–245.

Krutchinsky, A.N., Chernushevich, I.V., Spicer, V.L., Ens, W., and Standing, K.G. (1998). Collisional damping interface for an electrospray ionization time-of-flight mass spectrometer. J. Am. Soc. Mass Spectrom. *9*, 69–579.

Landrieux, E., Alic, N., Ducrot, C., Acker, J., Riva, M., and Carles, C. (2006). A subcomplex of RNA polymerase III subunits involved in transcription termination and reinitiation. EMBO J. *25*, 118–128.

Lorenzen, K., Versluis, C., van Duijn, E., van den Heuvel, R.H.H., and Heck, A.J.R. (2007). Optimizing macromolecular tandem mass spectrometry of large non covalent complexes using heavy collision gases. Int. J. Mass Spectrom., in press. Published online June 20, 2007. 10.1016/j.ijms.2007.06.012.

McCammon, M.G., Hernandez, H., Sobott, F., and Robinson, C.V. (2004). Tandem mass spectrometry defines the stoichiometry and quaternary structural arrangement of tryptophan molecules in the multiprotein complex TRAP. J. Am. Chem. Soc. *126*, 5950–5951.

McKay, A.R., Ruotolo, B.T., Ilag, L.L., and Robinson, C.V. (2006). Mass measurements of increased accuracy resolve heterogeneous populations of intact ribosomes. J. Am. Chem. Soc. *128*, 11433–11442.

Robinson, C.V. (2002). Protein complexes take flight. Nat. Struct. Biol. *9*, 505–506.

Ruotolo, B.T., and Robinson, C.V. (2006). Aspects of native proteins are retained in vacuum. Curr. Opin. Chem. Biol. *10*, 402–408.

Sadhale, P.P., and Woychik, N.A. (1994). C25, an essential RNA polymerase III subunit related to the RNA polymerase II subunit Rpb7. Mol. Cell. Biol. *14*, 6164–6170.

Schramm, L., and Hernandez, N. (2002). Recruitment of RNA polymerase III to its target promoters. Genes Dev. *16*, 2593–2620.

Sentenac, A. (1985). Eukaryotic RNA polymerases. CRC Crit. Rev. Biochem. *18*, 31–90.

Synowsky, S.A., van den Heuvel, R.H., Mohammed, S., Pijnappel, P.W., and Heck, A.J. (2006). Probing genuine strong interactions and post-translational modifications in the heterogeneous yeast exosome protein complex. Mol. Cell. Proteomics *5*, 1581–1592.

Tahallah, N., Pinkse, M., Maier, C.S., and Heck, A.J. (2001). The effect of the source pressure on the abundance of ions of noncovalent protein assemblies in an electrospray ionization orthogonal time-of-flight instrument. Rapid Commun. Mass Spectrom. *15*, 596–601.

van den Heuvel, R.H., and Heck, A.J. (2004). Native protein mass spectrometry: from intact oligomers to functional machineries. Curr. Opin. Chem. Biol. *8*, 519–526.

van den Heuvel, R.H., van Duijn, E., Mazon, H., Synowsky, S.A., Lorenzen, K., Versluis, C., Brouns, S.J., Langridge, D., van der Oost, J., Hoyes, J., and Heck, A.J. (2006). Improving the performance of a quadrupole time-of-flight instrument for macromolecular mass spectrometry. Anal. Chem. *78*, 7473–7483.

van Duijn, E., Bakkes, P.J., Heeren, R.M., van den Heuvel, R.H., van Heerikhuizen, H., van der Vies, S.M., and Heck, A.J. (2005). Monitoring macromolecular complexes involved in the chaperonin-assisted protein folding cycle by mass spectrometry. Nat. Methods *2*, 371–376.

van Duijn, E., Simmons, D.A., van den Heuvel, R.H., Bakkes, P.J., van Heerikhuizen, H., Heeren, R.M., Robinson, C.V., van der Vies, S.M., and Heck, A.J. (2006). Tandem mass spectrometry of intact GroEL-substrate complexes reveals substrate-specific conformational changes in the trans ring. J. Am. Chem. Soc. *128*, 4694–4702.

Wang, Z., and Roeder, R.G. (1997). Three human RNA polymerase III-specific subunits form a subcomplex with a selective function in specific transcription initiation. Genes Dev. *11*, 1315–1326.

Werner, M., Hermann-Le Denmat, S., Treich, I., Sentenac, A., and Thuriaux, P. (1992). Effect of mutations in a zinc-binding domain of yeast RNA polymerase C (III) on enzyme function and subunit association. Mol. Cell. Biol. *12*, 1087–1095.